J Therm Anal Calorim (2010) 101:815–821
DOI 10.1007/s10973-010-0745-5

Phase transformation in a nanostructured M300 maraging steel obtained by SPS of mechanically alloyed powders

C. Menapace · I. Lonardelli · A. Molinari

Received: 30 January 2009 / Accepted: 4 March 2010 / Published online: 27 March 2010
© Akadémiai Kiadó, Budapest, Hungary 2010

Abstract A Maraging M300 steel was produced by ball milling of elemental powders and Spark Plasma Sintering (SPS) consolidation at two different temperatures (950 and 1050 °C). Two types of nanostructured steels have been obtained. Thermal behaviors of these steels were investigated by means of Differential Scanning Calorimetry (DSC) and Dilatometry. Data provided by the two different techniques were seen to be in good agreement. A difference between the behaviors of the steel sintered at 950 °C and that sintered at 1050 °C was observed, due to the material sintered at lower temperature being more reactive to the intermetallics precipitation and austenite reversion on heating. On cooling, it shows a single martensite start temperature (Ms), whereas the steel sintered at 1050 °C shows a double peak for Ms.

Keywords Age hardening · Dilatometry · DSC · Nanostructured maraging steel

Introduction

Maraging steels are a class of ultra-high strength steels developed mainly for aerospace, aircraft and tooling application [1]. The name maraging derives from "martensite-aging," referring to the heat treatment carried out to induce the precipitation of intermetallics [2–5] in the Fe–Ni martensitic matrix, responsible for the excellent mechanical properties. Aging is carried out in the range 400–550 °C, and a prolonged exposure above 500 °C causes the reversion of martensite to austenite [6, 7], which leads to overaging.

In a previous article [8], the age-hardening behaviors of two nanostructured maraging steels obtained via mechanical alloying of powders and their consolidation by Spark Plasma Sintering (SPS) at 950 and 1050 °C were extensively analyzed. Both the steels display a very rapid aging kinetic in the so-called "early stages" of aging, i.e., the initial part of aging process, when precipitates are still in the coherent phase. The initial hardness increase was very consistent after just 30 s of aging. Moreover the peak hardness reached in the material sintered at 950 °C is higher than in a conventional M300. Over-aging kinetics was also investigated; it is faster than in a conventional wrought maraging steel, too. This aging behavior was ascribed to the nanostructure of the steels. In fact, the very low grain size, i.e., very high grain boundary surface, together with a consistent amount of crystalline defects (dislocation density) promotes the nucleation of the coherent precipitates [9, 10].

Since the age-hardening behavior depends on the transformations occurring on heating, they have been investigated by means of thermal analysis. Two different techniques, Differential Scanning Calorimetry (DSC) and Dilatometry (DIL) were used. All the transformations involved were analyzed, in relation to the three different steps of the aging curve (early stages of aging, maximum hardness, over-aging). The behaviors of the two nanostructured materials was compared, when possible, with the age-hardening response of a conventional wrought 18Ni300 maraging steel.

C. Menapace (✉) · I. Lonardelli · A. Molinari
Department of Materials Engineering and Industrial Technologies, University of Trento, via Mesiano 77, 38050 Trento, Italy
e-mail: cinzia.menapace@ing.unitn.it

Experimental Procedure

The powder of 18Ni300 maraging steel was obtained through mechanical alloying of elemental powders according to the composition reported in Table 1. The powders were ball milled for 20 h in a planetary mono-mill and then consolidated in a SPS apparatus at two temperatures (950 and 1050 °C) with a holding time of 1 min, using graphite punches and dies. Disks of 30 mm diameter and 5 mm height were prepared.

The SPS process is a pressure assisted pulsed current sintering process, based on the electrical spark discharge phenomenon: a high-energy, low-voltage spark pulse current that generates spark plasma at high localized temperatures, between the particles. The SPS process concentrates high-energy pulses in the gap between the powder particles offering significant improvements over conventional hot-pressing and hot isostatic pressing.

The sintering cycle used in this study consisted of heating under vacuum at 100 °C/min up to the sintering temperature and a holding at this temperature for 1 min. A pressure of 60 MPa was applied from 550 °C. Free cooling followed. Temperature was measured by a K-thermocouple inserted into the die.

Microstructural characterization was carried out at Light Optical Microscope (LOM) and by means of X-Ray Diffraction (XRD) analysis. The diffraction patterns were collected using a Cu kα source ($\lambda = 1.5418$) and an image plate detector over the 2-theta interval that ranges between 30 and 90°. The experimental spectra were analyzed using Rietveld method implemented in the Materials Analysis Using Diffraction (MAUD) software.

Phase transformations occurring during heat treatments were studied by means of Differential Scanning Calorimetry (DSC) and Dilatometry, using a Netzsch STA 409 Luxx apparatus and a Baehr Dylatometer DIL 805A/D. In both cases, a protective atmosphere was used (Ar/5%H2). The thermal cycle applied consists of heating at 20 °C/min up to 820 °C (the typical solution annealing temperature), isothermal holding for 1 h, and cooling with different rates: 10 °C/s in dilatometer, free in DSC, which is not equipped for rapid cooling.

Results

Powder

The mechanically alloyed powder is reported in Fig. 1. Sieve analysis indicated that the mean powder particle size is quite high, about 160 μm. The complete powder characteristics were published in a previous article [8]. XRD revealed that the powder is constituted by a BCC Fe–Ni martensite with a mean crystallite size of 15 nm. Microhardness is 670 $HV_{0.05.}$ Some carbon (0.068%wt.) and oxygen (0.25%wt.) contamination occurred during milling (from the balls and the jar made of steel) and the handling of the powder in air.

Table 1 Composition of the mix of powders ball milled to obtain the maraging powder

	Fe	Ni	Mo	Co	Ti	Al
Weight %	67.2	18	5	9	0.7	0.1

Density, microhardness and microstructure of SP Sintered steel

After consolidation via SPS, the disks have the density, microhardness and mean crystallite size of the bcc martensite reported in Table 2 [8].

LOM micrographs of the consolidated samples are reported in Fig. 2(a–b) in which the different amounts of pores are clearly evident. The microstructure is very fine and cannot be resolved under LOM. White lines in Fig. 2b are Mo_2C particles formed during sintering [8], preferentially at the original powder particles surface, due to the carbon contamination. Their amounts are very low at 950 °C, and much higher at 1050 °C.

Study of aging

Early stages of aging

As already mentioned, aging of the nanostructured M300 steel is characterized by an extremely rapid hardness increase in the early stages characterized by the coherent precipitation. This hardness increase is higher for SPS950, relative to SPS1050. Compared to that of a conventional

Fig. 1 Maraging powder particles after 20 h milling

Table 2 Relative density of the SP Sintered disks

Code	SPS temperature/°C	Relative density/%	Microhardness/$HV_{0.05}$	Mean crystallite size/nm
SPS950	950	96	456	36
SPS1050	1050	99.7	423	47

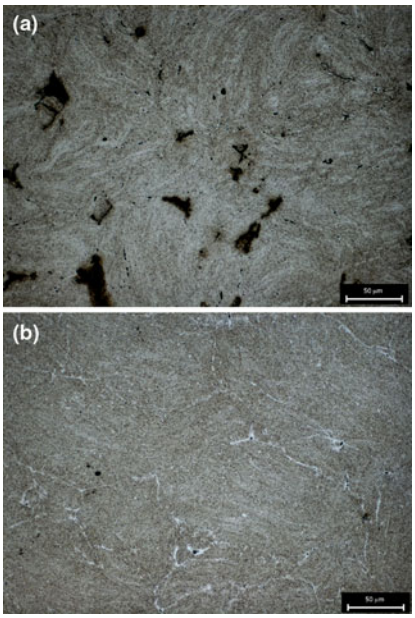

Fig. 2 Microstructure of the materials SP Sintered at 950 (**a**) and 1050 °C (**b**)

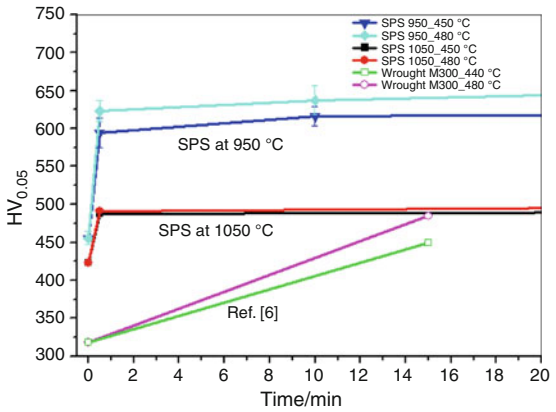

Fig. 3 Initial stages of aging in M300 obtained through ball milling and SPS consolidation and in a conventional wrought M300 steel

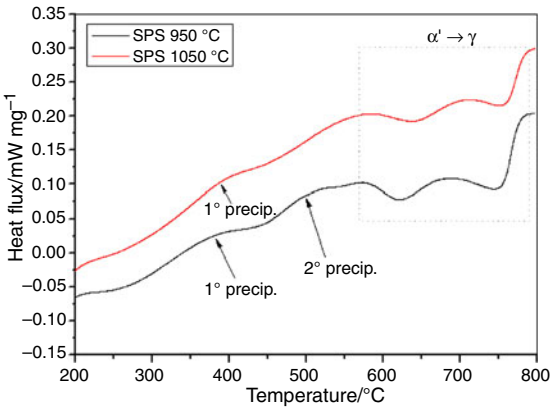

Fig. 4 DSC curves of 950 and 1050 °C SP Sintered samples (heating step)

wrought M300 (Fig. 3), the initial hardness increase of the nanostructured steels is much more rapid and, in the case of SPS950, hardness is also much higher. After 30 s aging, 594 $HV_{0.05}$ and 623 $HV_{0.05}$ were obtained at 450 and 480 °C, respectively, with an increased hardness relative to the as sintered condition of 138 and 167 $HV_{0.05}$. The conventional M300 shows the same hardness increase after 15 min of aging [6] or even more [11], indicating a much slower hardening process.

The early stages of aging are related to the precipitation of intermetallic compounds that, at the beginning, are in a coherent form. Precipitation can be observed through the DSC analysis, as reported in Fig. 4.

The DSC heating curve is characterized by two (SPS950) and one (SPS1050) exothermic peaks at 350–550 °C, followed by two endothermic peaks (framed in the figure) starting at 600 °C. The first peaks are due to the intermetallics precipitation; the two following endothermic peaks are due to the reversion of martensite to austenite, that occurs in two steps if the heating rate is not too high [12]. DSC data are summarized in Table 3.

SPS950 shows all the peaks (precipitation, $\alpha' \rightarrow \gamma$ reversion) at lower temperatures with respect to SPS1050. This is indicative of a higher reactivity of this steel due to its lower grain size and the higher amount of defects that promote both the intermetallic precipitation and the nucleation of austenite from martensite.

In order to understand the different precipitation occurring in the materials SPS950 and SPS1050 an X-Ray analysis was carried out on samples heated at different temperatures and rapidly quenched in order to "freeze" the microstructure. The temperatures chosen for these analyses were 460 and 570 °C, respectively, at the end of the first precipitation peak (that is common for both the materials) and after the second peak, detected only in SPS950 steel. The results are reported in Fig. 5. It was observed in both materials the presence of Ni_3(Ti, Mo) precipitates and the formation of $FeMo_2$ only in the SPS950 material heated at

Table 3 Data derived from DSC curves

SPS temperature/°C	Precipitation start *T*/°C	Precipitation finish *T*/°C	Second precipitation interval	Austenite start *T*/°C	Austenite second step start *T*/°C	Austenite finish *T*/°C
950	288	461	460–570 °C	594	706	767
1050	296	480	Not detected	606	727	777

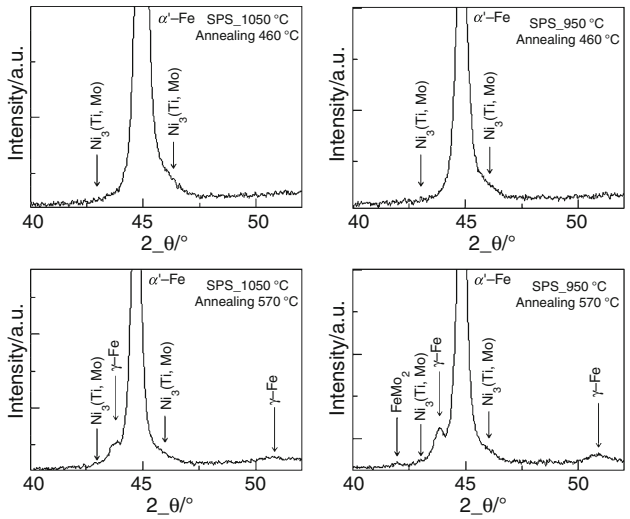

Fig. 5 X-Ray diffractograms (only the region of interest is reported) carried out at RT, on materials SPS950 and SPS1050 heat treated at 460 and 570 °C. The intensities are in arbitrary units

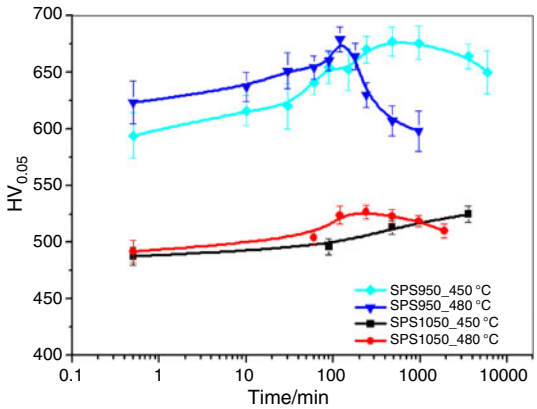

Fig. 6 Aging curves at 450 and 480 °C of the two materials

570 °C. Therefore, the precipitation of this intermetallic can be correlated to the second precipitation peak observed in the calorimetric curve of the SPS950 material. $FeMo_2$ was not observed in the SPS1050 material because of the lack of molybdenum, which forms the carbide network shown in Fig. 2b. The more extensive precipitation observed in SPS950 material is responsible for the larger increase in hardness in this type of this steel than in SPS1050.

In the X-Ray spectra of the materials treated at 570 °C, some austenite is visible, indicating that reversion to austenite has been already initiated at this temperature.

Peak hardness

Aging curves at 450 and 480 °C of the two materials are illustrated in Fig. 6. Hardness of SPS950 is much higher than that of SPS1050 over the whole aging range, and the maximum hardness of the two materials differs by about 150 Vickers at the aging temperature of 480 °C. This cannot be simply related to the different crystallite sizes, since they are quite nearly the same (36 vs. 47 nm), but it is due to the different precipitation phenomena, as explained above. Age-hardening curves allow the calculation of the activation energy for precipitation to be made [8]; the activation energies are 150 kJ/mole and 269 kJ/mole for SPS950 and SPS1050, respectively. The smaller the activation energy of the material with the smaller crystalline size the faster the precipitation, because of the effect of structural defects on diffusion. This confirms what was previously discussed with reference to the early stage of aging.

The deviations in hardness are related to a different contents of Mo in the matrix. It influences also the matrix Martensite Start temperature (Ms), which was determined by dilatometry. The cooling part of the dilatometric curves and the first derivative of the dimensional change used for Ms determination are depicted in Fig. 7a and b, respectively. Ms is individuated as the point in which the first derivative starts to increase, as indicated in the figure. The value of Ms is 178 °C for SPS950, and this Ms value of this material found by dilatometry is in good agreement with the value found by DSC (i.e., 184 °C), and both are in good agreement with Ms of a wrought 18% Ni maraging steel. On the contrary, maraging sintered at higher temperature has a Ms of 241 °C but shows a double peak, the first set at 216 °C and the second at 210 °C, as shown in Fig. 7b. This peak shape was recorded also by DSC, as shown in Fig. 8.

The Ms of SPS950 maraging and the second Ms peak of SPS1050 steel can be considered equivalent and representative of the martensite transformation temperature of these steels. The first Ms peak of 1050SPS (at about 240 °C) is attributed to the inhomogeneity of the microstructure. In this material, in fact, as previously described, a

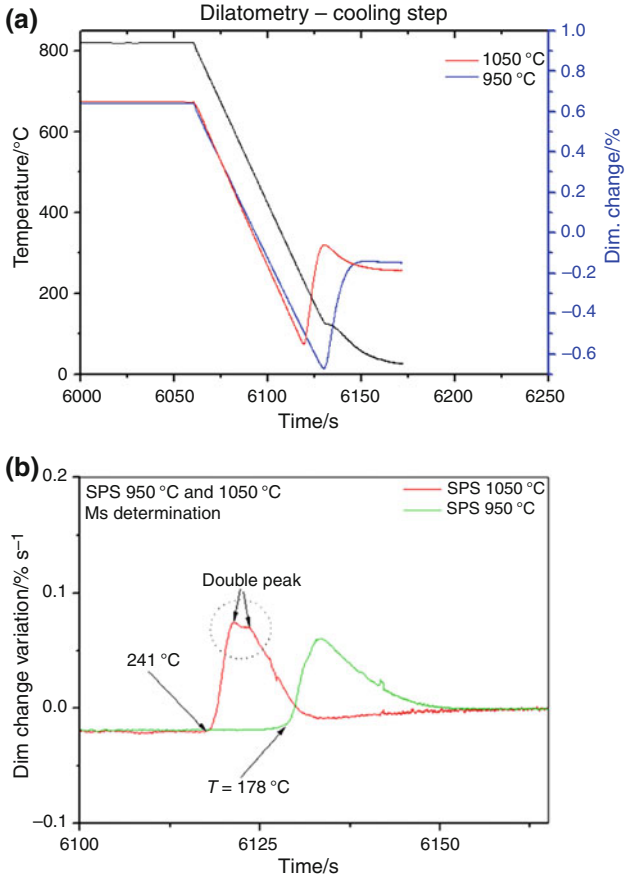

Fig. 7 **a** Cooling step of dilatometric curves of materials SP Sintered at 950 and 1050 °C; (**b**) first derivative of dimensional change used for Ms determination

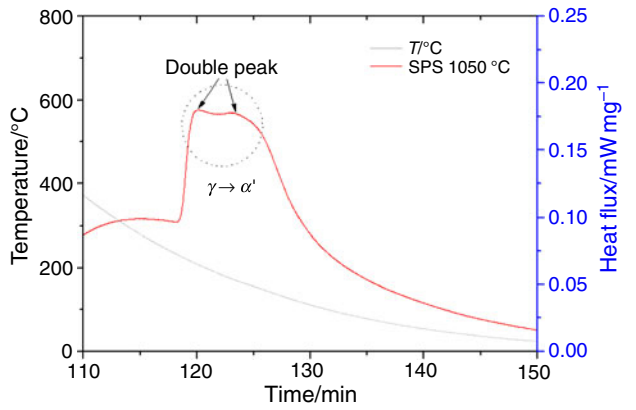

Fig. 8 Martensite formation peak in DSC curve of material sintered at 1050 °C

Mo_2C network formed during sintering. Near these carbides, the molybdenum content is probably lower, and so these areas possess a higher Ms since molybdenum, as well as all the other elements except cobalt, decrease Ms of maraging steels [1].

Overaging

Figure 9 compares the 480 °C aging curves of the nanostructured steels and of a wrought one, to focus attention on overaging, which is characterized by a decrease of hardness with aging time. Hardness of SPS950 and SPS1050 decrease after aging time of 2 and 4 h, respectively, whilst that of the reference steel is still increasing after 10 h. In addition, overaging rate is much higher in SPS950. Overaging is modeled by Wilson [13] with the following equation:

$$\left(\frac{1}{\Delta H}\right)^3 = M(t - t_0) + \left(\frac{1}{\Delta H_0}\right)^3$$

where ΔH is the hardness difference between the overaged sample and the solutionized one; M is the temperature-dependent rate constant; t_0 is the time of the maximum hardness, and ΔH_0 is the hardness increase at the commencement of coarsening time (i.e., initial stage of overaging). M values of the two nanostructured materials are quite similar (1.64×10^{-8} vs. 2.2×10^{-8}) [8], despite the evident difference shown by Fig. 8. The model, in fact, tends to reduce the importance of the first stage of overaging. By calculating the slope of the aging curves at the beginning of overaging (i.e., in the first 200 min), two extremely different rates are found: 0.33 kgf/mm min^{-1} and 0.007 kgf/mm^2 min^{-1} for the SPS950 and SPS1050, respectively.

The effect of nanostructure on the overaging kinetics is confirmed by comparison with literature data relevant to a wrought M300. Figure 10 shows the overaging steps of SPS1050 and of the reference material at 510 °C; the overaging rates are −0.027 kgf/mm^2 min^{-1} and −0.017 kgf/mm^2 min^{-1}, respectively.

Overaging is due to coarsening of precipitates and to reversion to austenite of the martensitic matrix. This

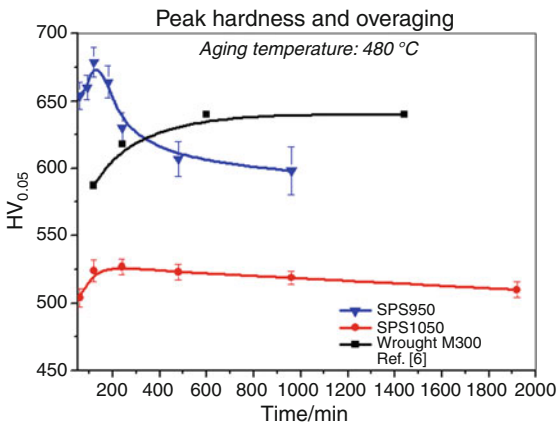

Fig. 9 Maximum hardness and overaging at 480 °C of M300 SP Sintered at 950, 1050 °C and a wrought M300

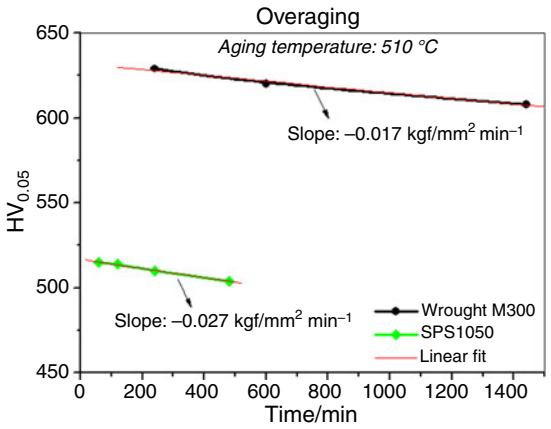

Fig. 10 Overaging part of aging curves at 510 °C of the maraging steel SP Sintered at 1050 °C and a wrought M300

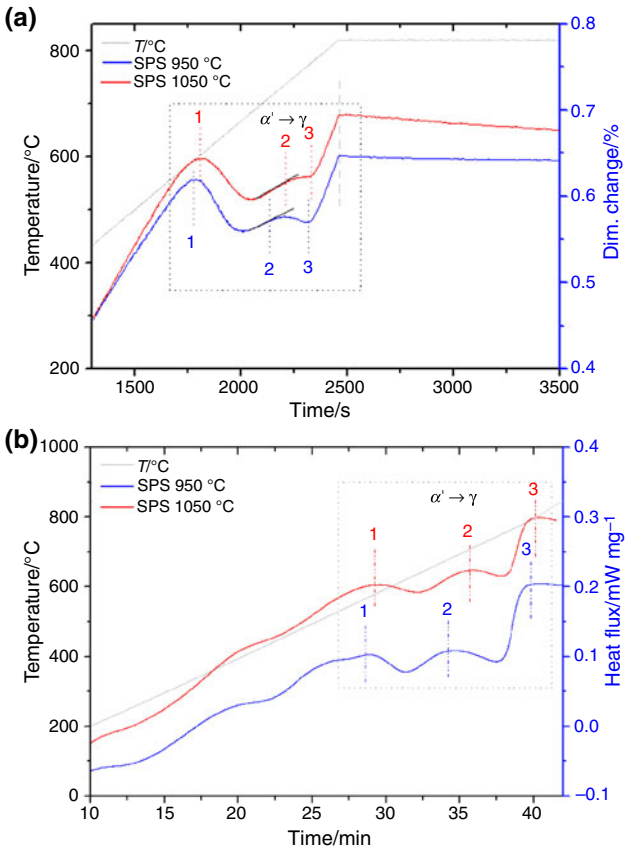

Fig. 11 Dilatometric curves (**a**) and DSC curves (**b**) of maraging steels SP Sintered at 950 and 1050 °C indicating the reversion of martensite to austenite on heating

transformation is reported to occur at 630 °C in a wrought M300 steel [14]. In the nanostructured steels investigated here, it occurs at a lower temperature, as shown by DSC and dilatometric curves shown in Fig. 11a and b and by X-Ray analysis, confirming the tendency of a faster over-aging than in wrought steel. Transformation is split into two steps, indicated by points 1, 2, and 3 in the figures (1 = beginning of the first peak, 2 = beginning of the second peak, 3 = end of the second peak). The two consecutive peaks are observed since the use of low heating rate (20 °C/min) leads to a partitioning of the matrix into Ni-rich and Ni-poor areas, having different Austenite start temperature. The first step of $\alpha' \rightarrow \gamma$ transformation is a predominantly diffusive process [11] and therefore occurs only if the heating rate is quite low, whereas the second one is a diffusionless shear transformation that occurs at every heating rate.

Table 4 Dilatometric data on reversion to austenite of steels sintered at 950 and 1050 °C

SPS temperature/°C	$\alpha' \rightarrow \gamma$ start temperature/°C	$\alpha' \rightarrow \gamma$ second step start temperature/°C	$\alpha' \rightarrow \gamma$ end temperature/°C
950	591	720	772
1050	604	740	780

Temperatures detected by dilatometry, listed in Table 4, agree quite well with those drawn from DSC (Table 3), and are significantly lower in SPS950 than in SPS1050. As for intermetallics precipitation, reversion to austenite is activated by the finer grain size of martensite.

Conclusions

The age-hardening behavior of two nanostructured 18Ni300 maraging steels obtained by mechanical alloying of elemental powders and SPS consolidation was analyzed by means of thermal analysis. The age-hardening curve was divided into three parts: early stage of aging, peak hardness, and overaging. Each part was examined considering the relevant phase transformations.

Both intermetallics precipitation and austenite reversion occur at lower temperatures in the cases of maraging steels than in wrought steel, and temperature decreases with the grain size. Thus, nanostructure enhances both age hardening and overaging, because of the effect of the structural defects on diffusion and austenite nucleation.

Carbon contamination during mechanical alloying is quite negative for this kind of steel, since it causes the precipitation of Mo carbides on sintering. These carbides deplete the martensitic matrix from Mo, thus reducing the intermetallic precipitation and, in turn, age hardening. The lower the SPS temperature, the less the amount of carbides precipitated. Carbides precipitation was detected by the microstructural characterization and confirmed by X-Ray analysis. It has an effect on the martensitic transformation and, in particular, on Ms temperature.

References

1. ASM handbook, vol. 1. ASM International, Materials Park, OHIO, USA, 2005. pp. 1225–1237.
2. Decker RF, Floreen S. Maraging steels-the first 30 years. In: Wilson RK, editors. Maraging steels: recent developments and applications. The Minerals, Metals & Materials Society, Warrendale, Pennsylvania; 1988. p. 1.
3. Servant C, Lacombe P. Structural transformations produced during tempering of Fe–Ni–Co–Mo alloys. J Mater Sci. 1977; 12:1807–26.
4. Sha W, Cerezo A, Smith GDW. Phase chemistry and precipitation reactions in maraging steels: part I. Introduction and study of co-containing C-300 steel. Metall Trans A. 1993;24:1221–32.
5. Tewari R, Mazumder S, Batra IS, Dey GK, Banerjee S. Precipitation in 18 wt% Ni maraging steel of grade 350. Acta Mater. 2000;48:1187–200.
6. Pardal JM, Tavares SSM, Terra VF, Da Silva MR, Dos Santos DR. Modeling of precipitation hardening during the aging and overaging of 18Ni–Co–Mo–Ti maraging 300 steel. J Alloy Comp. 2005;393:109–13.
7. Peters DT. A study of austenite reversion during aging of maraging steels. Trans ASM. 1968;61:62.
8. Menapace C, Libardi S, D'Incau M, Molinari A. Advances in powder metallurgy & particulate materials. In Proceedings of PM2008, international conference on powder metallurgy and particulate materials, vol. 9, Washington 8–12 June 2008, MPIF, Princeton, New Jersey; 2008. pp. 402–406.
9. Wilson EA. Quantification of early stages of age hardening in Fe–12Ni–6Mn maraging type alloy. Mater Sci Tech. 1998;14:277–82.
10. He Yi, Yang Ke, Guo Zhanli, Liu Kai. Age hardening and mechanical properties of a 2400 MPa grade cobalt-free maraging steel. Metall Mater Trans A. 2006;37:1107–16.
11. Pektas I, Atala H. The effects of various heat treating parameters on the hardness and microstructures of the experimental 18% Nickel maraging steels. J Therm Anal Calorim. 1998;54:803–14.
12. Kapoor R, Kumar L, Batra IS. A dilatometric study of the continuous heating transformations in 18wt.% Ni maraging steel of grade 350. Mater Sci Eng A. 2003;352:318–24.
13. Wilson EA. Quantification of age hardening in an Fe–12Ni–6Mn alloy. Scripta Mater. 1997;36(10):1179–85.
14. Kladaric I, Krumer D, Markovic R. The influence of multiple-solution annealing on kinetics of structural transformation of maraging steels. Mater Manuf Process. 2006;21:783–5.